15556   FINE-GRAINED OLIVINE-NORMATIVE   ST. 9A   1542.0 g
                MARE BASALT

INTRODUCTION: 15556 is a medium-grained, extremely vesicular olivine-normative basalt containing small olivine phenocrysts. It is ~3.4 b.y. old. According to the Apollo 15 Lunar Sample Information Catalog (1972), a l-cm xenolith occurs on one face. A few percent yellow-green olivine phenocrysts are visible. The basalt is medium gray, subrounded (Fig. 1), and tough. The sample was barely in the soil, lacking fillets or much dust coating, and has zap pits on all surfaces.

15556 was collected approximately 60 m northeast of the rim of Hadley Rille, from an area in which rocks as large as 20 cm are common. Its orientation was documented.
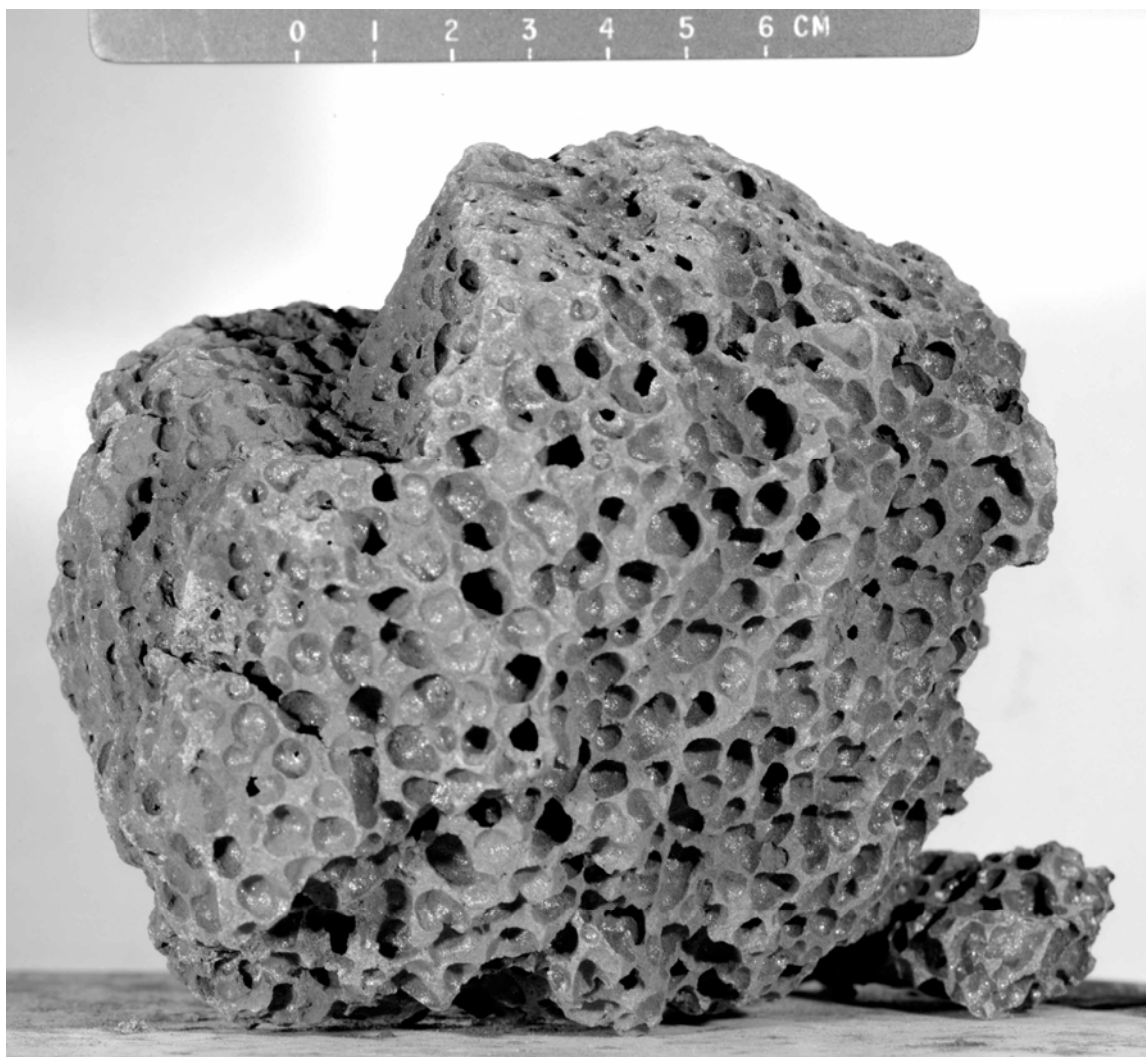

Figure 1. Macroscopic view of 15556, showing large vesicles on "B" side. S-71-45243

PETROLOGY: The sample is conspicuous because of its vesicles. They show a continuous change from one side of the rock to the other in both size and abundance, which both increase as the rock's apparent grain size decreases. However, thin sections reveal no conspicuous change in grain size across the rock (Fig. 2) although they do in vesicularity. There appear to be fewer and smaller olivine phenocrysts in those thin sections with more vesicles than in those with fewer vesicles. The largest vesicles are almost a centimeter across.

Little on the petrology of 15556 has been published. The Apollo 15 Sample Information Catalog (1972) gave a mode for thin section ,15 of 50% clinopyroxene, 30% plagioclase, 5% olivine, 5% cristobalite, 3% ilmenite, 3% ulvospinel, 2% chromite, 1% mesostasis, and traces of Fe-Ni metal and troilite. Rhodes and Hubbard (1973) reported a mode with 57% pyroxene, 38% plagioclase, and only 0.1% olivine.

Inspection of thin sections shows ragged, corroded olivines, and ragged laths of plagioclase which partly enclose generally granular, small clinopyroxenes (Fig. 2). Except for the size of vesicles, this texture is common across the sample. Brunfelt et al. (1973) made microprobe analyses of pyroxenes (Fig. 3) in conjunction with their chemical analyses of mineral separates. El Goresy et al. (1976) made analyses of spinels. The spinels occur as corroded and rounded chromite cores (inclusions) in Cr-ulvospinel; analyses are diagrammed in Figure 4. El Goresy et al. (1976) discussed the compositional zoning and substitutional trends. Engelhardt (1979) tabulated ilmenite paragenesis. Huffman et al. (1972, 1974, 1975) made Mossbauer and magnetic studies of 15556, finding clear evidence for olivine, and analyzing the distribution of Fe among phases. Huffman et al. (1975) interpreted the spectra as requiring subsolidus reheating of the sample for a long time at moderate temperatures.

Garvin et al. (1982) studied the physical properties (length, width, distance to nearest neighbor, etc.) of the vesicles, finding an average diameter of 4.1 mm. Calculations of the vesicle distribution are consistent with a magma ascending at 0.20 m/sec with 80 to 400 ppm dissolved CO. The magma rise rate is more influential in these calculations than is viscosity. These authors do not discuss the variation of vesicles across the sample.

EXPERIMENTAL PETROLOGY: Humphries et al. (1972) conducted low-pressure crystallization experiments on 15556 (Fig. 5). It has a high-temperature olivine liquidus, with pigeonite the second silicate phase to crystallize. The sample is substantially crystalline at anorthite crystallization. They prefer the interpretation that the sample is not a liquid composition, but a mafic cumulate.

CHEMISTRY: Chemical analyses are listed in Table 1, with rare earths shown in Figure 6. The analyses, which generally are not specifically discussed by their authors, are quite consistent with each other and have the high iron and titanium of Apollo 15 olivine-normative basalts. According to the low MgO, it is a fairly evolved member of the group. Rhodes (1972) analyzed split ,5 but did not publish the analysis, using it only in an average of olivine-normative basalts. Brunfelt et al. (1973) also reported mineral separates data for plagioclase, pyroxene, and olivine.
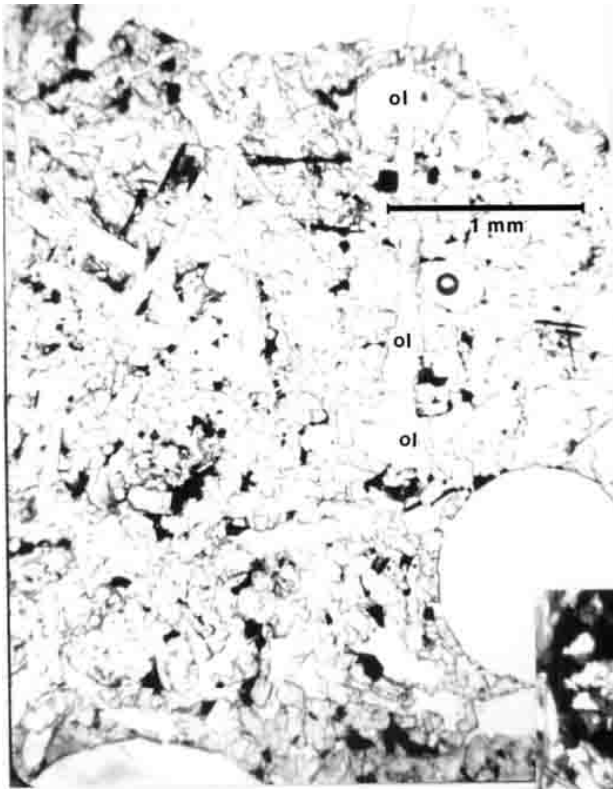
Figure 2. Photomicrographs of thin sections, all to same scale
(a) 15556,132 from one end with small vesicles, transmitted light;
(b) as (a) crossed polarizers. "ol" is a single, corroded olivine grain;
(c) 15556,130, from other end, with large vesicles (not shown), transmitted light;
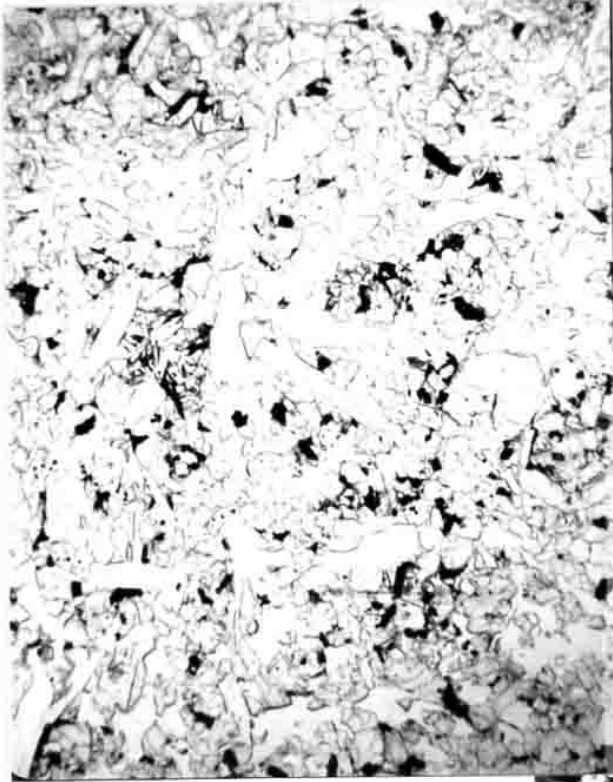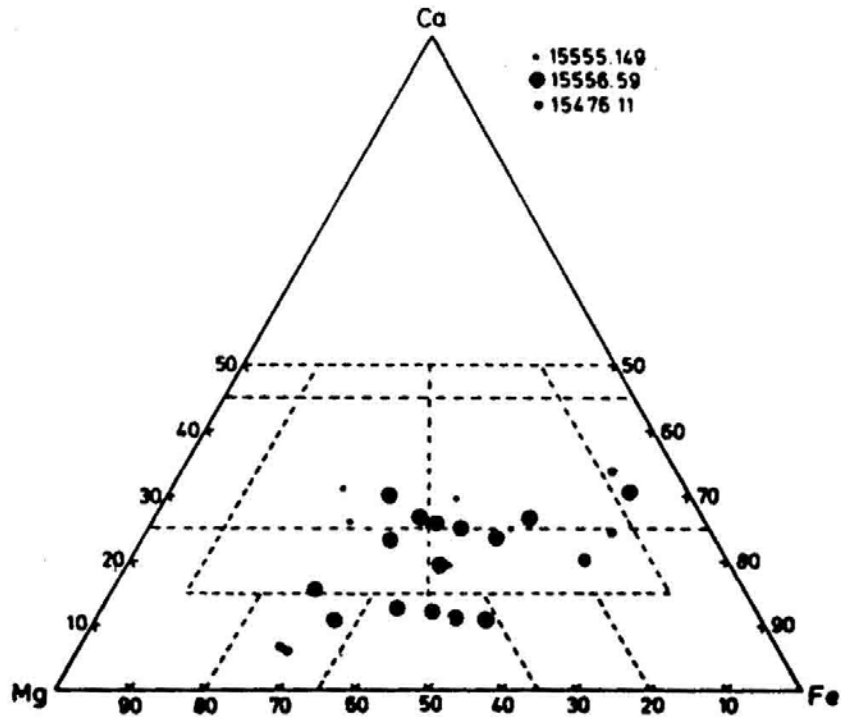(d) as (c) crossed polarizers.

Fig. 2c

Fig. 2d

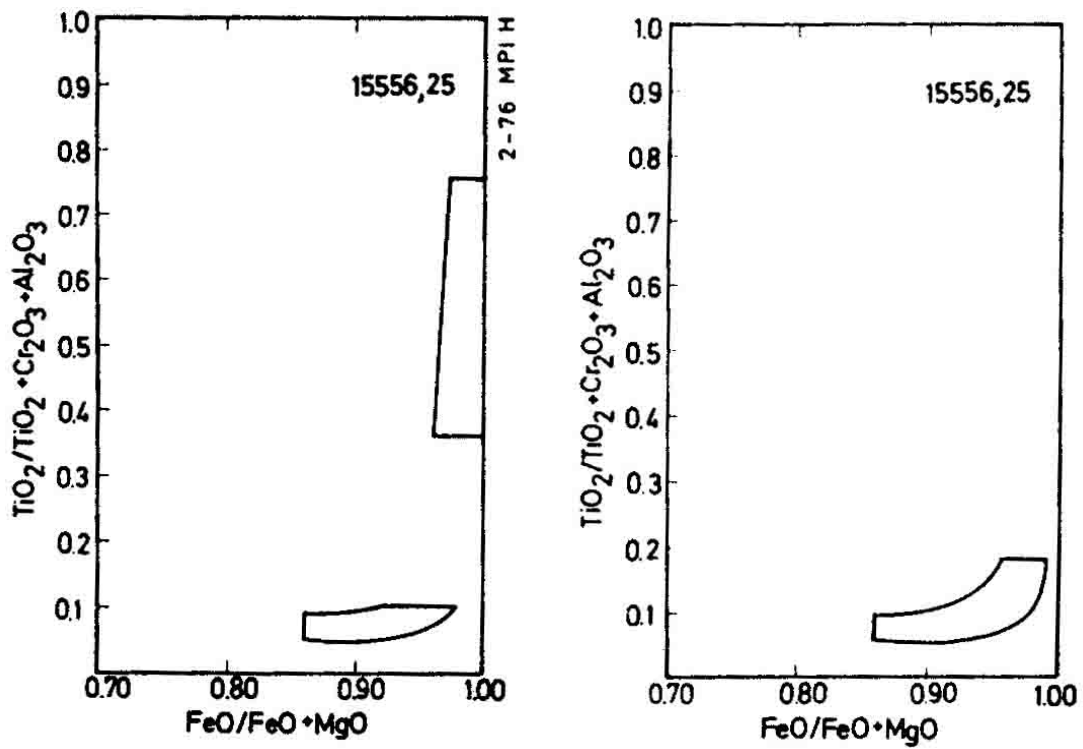Figure 3. Pyroxene compositions (Brunfelt et al., 1973).

Figure 4. Compositions of spinels (El Goresy et al., 1976).

Ganapathy et al. (1973) noted a strong enrichment in Cd (~10x) over other Apollo 15 mare basalt samples, and suggested that Cd was in the gas phase which gave the rock its vesicularity. They also profess doubt on their Rb analysis, but only because it differs from that reported by other laboratories. Muller (1976) cited the disparity between his nitrogen analyses as a probable result of sample heterogeneity, although both sets were on the same split ,25.

Desmarais et al. (1974) found a H concentration of 4 micromoles/ gm (pyrolysis), much lower than soils. The H is even lower than other mare basalts, consistent with outgassing manifested in the vesicularity. Gibson et al. (1975) analyzed for CO, CO_2, H_2, H_2S , and metallic iron. Gibson and Andrawes (1978) analyzed gas released on crushing the sample, finding no active gases, e.g. nitrogen less than 10 ppm.

Goldberg et al. (1976) analyzed for F in the surfaces of vesicle and inter-vesicle areas, in a study aimed at determining the composition of the gas which formed the vesicles. They found more F in the vesicles than in inter-vesicle areas for fresh-sawn samples. The vesicle F abundance is still ~10x less than on Apollo 15 Green Glass, a result of either different gas compositions or more efficient condensation on the faster-cooled glass. Neither F or S would have enough total pressure to have formed the vesicles, the gas for which they believe to have been mainly CO.

STABLE ISOTOPES: Clayton et al. (1974) reported oxygen isotope analyses for mineral separates (Table 2). The data is consistent with fractionation at temperatures of ~1100°C.

Gibson et al. (1975) reported typically magmatic sulfur isotopes ($\delta^{34}S$) of +0.9. Lipschutz et al. (1973) reported a $^{50}V/^{51}V$ isotopic ratio, in part of a search for early, energetic charged particle radiations. Strasheim et al. (1972) reported a $^{7}Li/^{6}Li$ ratio of 12.2.

RADIOGENIC ISOTOPES AND GEOCHRONOLOGY: Kirsten et al (1972) analyzed Ar isotopes and found a total K-Ar age of 3.4 ± 0.1 b.y. Temperature releases were not reported. [Strasheim et al. (1972) stated that the $^{7}Li/^{6}Li$ relation leads to an age of 3.05 b.y., but no details of the "method" were given.]

RARE GASES AND EXPOSURE: Kirsten et al. (1972) reported rare gas isotopic data and found consistent exposure ages from three methods: ^{3}He 490 ± 50 m.y., ^{21}Ne 525 ± 40 m.y., ^{38}Ar 490 ± 50 m.y. Rancitelli et al. (1972) measured cosmogenic radionuclides, finding a long exposure relative to the ^{26}Al halflife. The sample has a high $^{26}Al/^{22}Na$ ratio in comparison with other mare basalts, perhaps because it had been barely buried in the lunar regolith.

PHYSICAL PROPERTIES: Nagata et al. (1972a,b, 1973, 1974) reported basic magnetic and NRM data for ,37 and ,38 (Figs. 7-9). Unlike most other basalts, kamacite with a few per cent nickel rather than metal almost lacking Ni appears to be the major ferromagnetic phase. ,38 was split into two parts, one black, the other gray. The black has a strong NRM, and the gray a weak NRM similar to ,37, also gray. The NRM has a hard

component ~1x10^{-6} emu/gm, with a direction reasonably invariant for AF demagnetizing fields greater than 100 Oe.rms (Figs. 8, 9). Partial thermo-remanent magnetization increases steadily with temperature to 800°C, and if the stable component of NRM can be attributed to PTRM, an ambient lunar field of 3400 gammas (Nagata et al. 1973) or ~2000 gammas (Nagata et al. 1972b) is implied. Schwerer and Nagata (1976) applied the technique of magnetic granulometry to the published magnetic data, tabulating distribution parameters for fine-grained (30-150 Å) metallic iron. Brecher (1975, 1976) listed 15556 under two sections of her lists of samples which show "textural remanence."
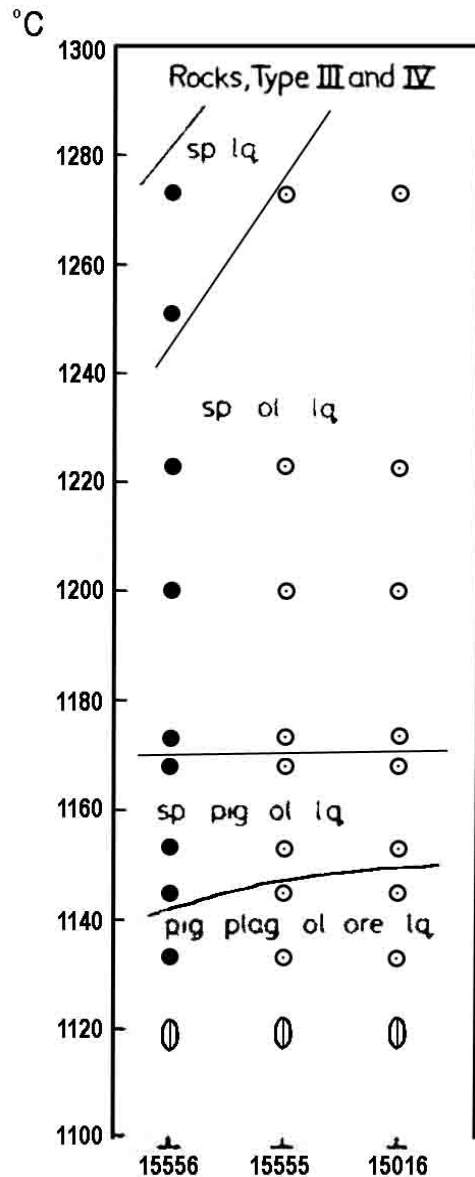
Figure 5. Low-pressure crystallization, black dots (Humphries et al. , 1972) .

Gold et al. (1974, 1975, 1976) made Auger spectra of pulverized rock, finding that pulverized rock has a higher albedo than soils because the soil grains have more iron in their surfaces. Solar wind simulation experiments, with s-particles in the case of 15556, caused an increase in Fe/O and Ca/O in surfaces (shown by Auger analysis). The experiments strongly support the model that selective sputtering of oxygen and other light elements by solar wind irradiation is the cause of lower albedo in soils.

Figure 6. Rare earths in bulk rock.

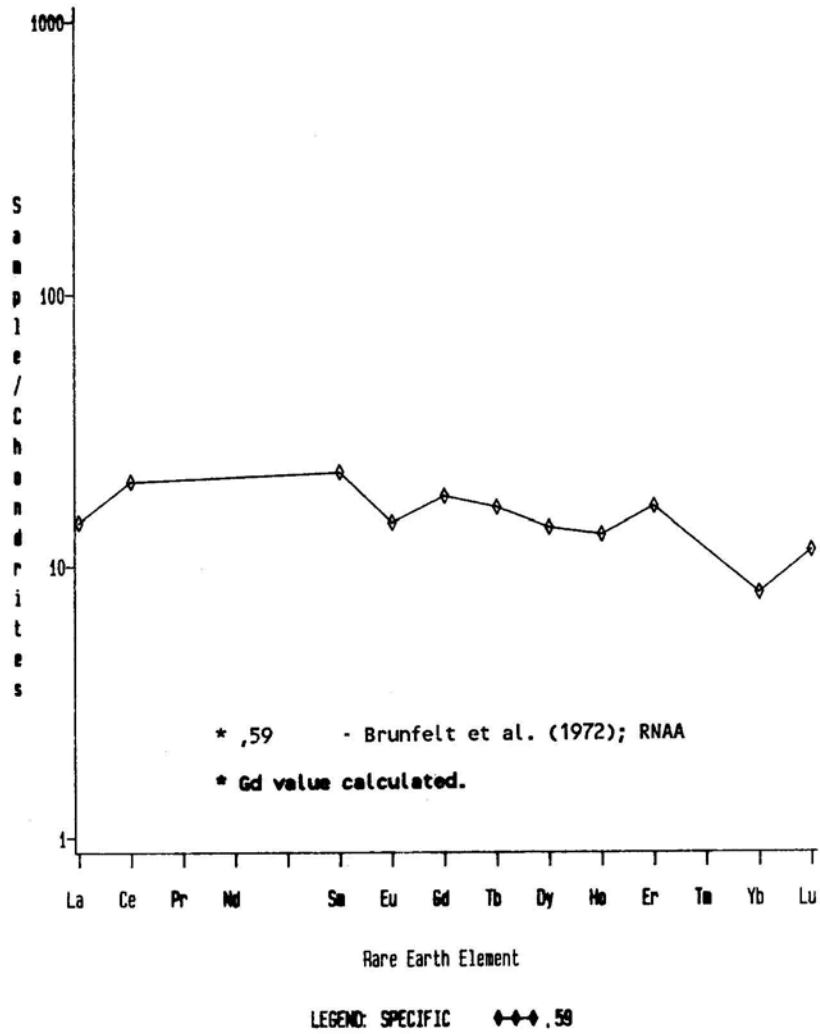TABLE 15556-1. Chemical analyses of bulk rock

		,26	,59	,25	,25	,12	,4	,9	,159	,125	,0
Wt. %	SiO_2	46.18				46.2					
	TiO_2	2.64	2.04			2.68					
	Al_2O_3	9.85	9.24			9.44					
	FeO	21.70	21.41			21.62					
	MgO	8.03		8.2		8.09					
	CaO	10.72	9.94	11.3		10.54					
	Na_2O	0.30	0.28	0.279c		0.22					
	K_2O	0.09		0.0470		0.06					0.053
	P_2O_5	0.07				0.08					
(ppm)	Sc		43.1								
	V	165	266			255					
	Cr	5200	3200			4300					
	Mn	2500	1800			2000					
	Co	46	50.3			49		51			
	Ni	65	50			57					
	Rb	<5	0.84	0.85		3		0.10a			
	Sr	102	88	103		96					
	Y	50				32					
	Zr	100				85					
	Nb					8					
	Hf		3.1								
	Ba	50	59	53		85					
	Th		0.40								0.56
	U		0.21	0.15				0.145			0.15
	Pb	<2									
	La		4.8	5.5							
	Ce		18								
	Pr										
	Nd										
	Sm		4.0								
	Eu		1.00								
	Gd										
	Tb		0.77								
	Dy		4.4								
	Ho		0.91								
	Er		3.3								
	Tm										
	Yb		1.59								
	Lu		0.39								
	Li	9		8.0							
	Be										
	B	3									
	C						16				
	N				<10					126	
	S								965b		
	F										
	Cl										
	Br							13			
	Cu	10	7.1			9					
	Zn		1.2					2.1			
(ppb)	I										
	At										
	Ga	5000	3700								
	Ge							9.8			
	As		<50								
	Se		106					142			
	Mo										
	Tc										
	Ru										
	Rh										
	Pd										
	Ag		<7					0.85			
	Cd							28			
	In		<2					0.56			
	Sn										
	Sb							0.13			
	Te							2.7			
	Cs		<32	30				32			
	Ta		400								
	W		430								
	Re							0.00413			
	Os										
	Ir		<0.1					0.039			
	Pt										
	Au		0.85					0.026			
	Hg										
	Tl							0.32			
	Bi							0.18			
		(1)	(2)	(3)	(4)	(5)	(6)	(7)	(8)	(9)	(10)

References and methods:

(1) Mason et al. (1972); varied
(2) Brunfelt et al. (1972); RNA
(3) Miller (1972a, 1975); AAS, RNA
(4) Miller (1972b); Kjeldahl method, "conventional"
(5) Strasheim (1972); Varied
(6) Moore et al. (1972, 1973)
(7) Ganapathy et al. (1973); RNA
(8) Gibson et al. (1975); Combustion
(9) Miller et al. (1976); Kjeldahl method, "optimized"
(10) Rancitelli et al. (1972); Gamma ray spectroscopy

Notes:

(a) Quoted by authors as probable analytical error (also Wolf et al., 1979).
(b) A lower value was obtained from hydrolysis
(c) Revised from (1972a) value.

TABLE 15556-2. Oxygen isotopes
(δ18 °/oo SMOW) (Clayton et al. 1972)

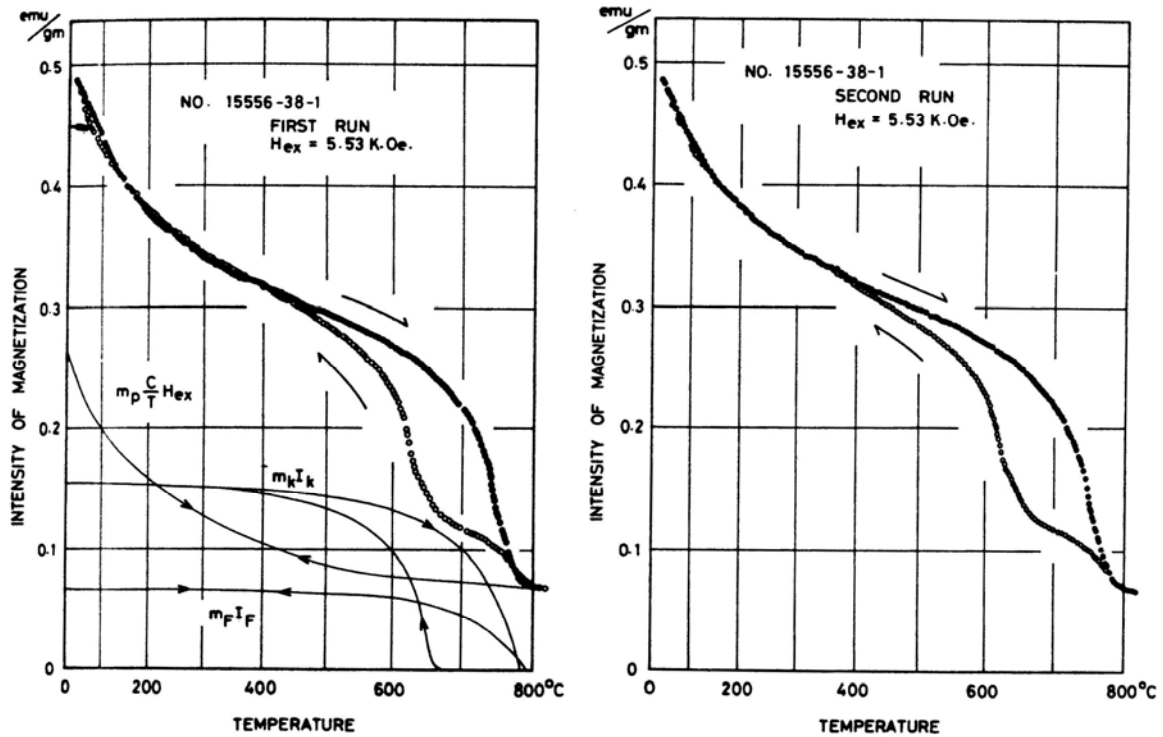|	Plag	Px	Ol	Ilm
,63	5.88	5.68	4.99	4.01

Figure 7. Magnetic hysteresis loops
(Nagata et al., 1974).

PROCESSING AND SUBDIVISIONS: Two chips ,1 (18.0 g) and ,2 (6.1 g) (which were loose in the bag with 15556 but fitted onto broken surfaces i.e. documented) provided the first allocations. Two potted butts ,3 and ,10, from ,2 and ,1 respectively, provided all the thin sections until a new slab was cut in 1981 (below). A saw cut was made through 15556 and the end piece dissected for allocation (Fig. 10). The remainder of ,36 is in remote storage. A few pieces were incorporated into educational disks. In 1981 a new saw cut (Fig. 10) was made from ,0 (now 1184.1 g) to produce thin sections directly relatable to the vesicularity variation (Table 3) and other sub-samples.
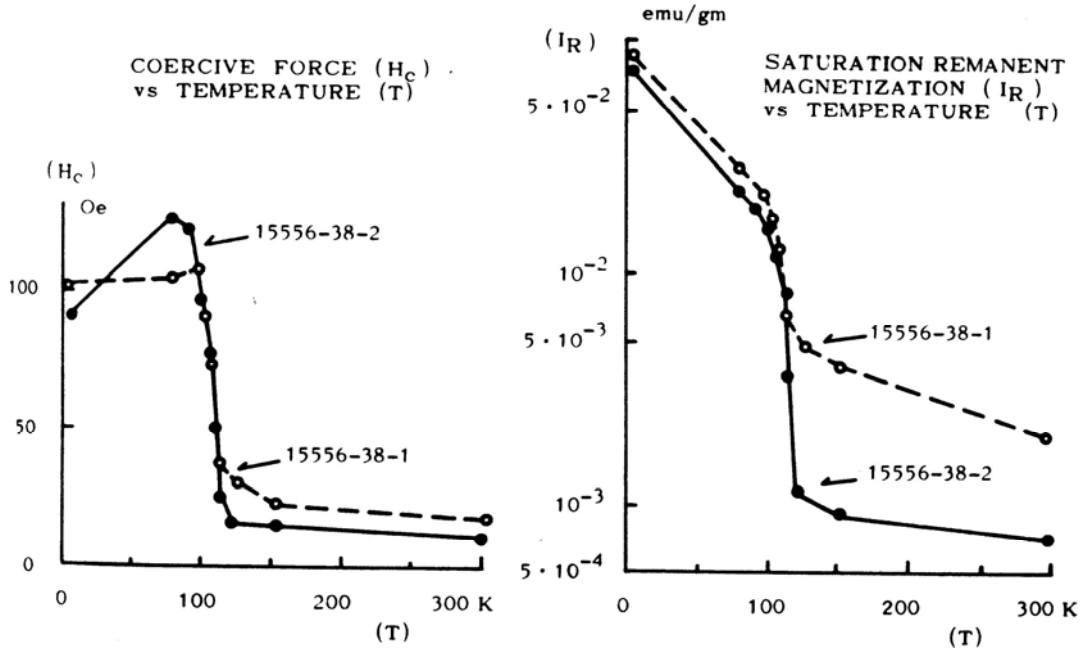
Figure 8. Dependence of the coercive force Lleit) and the saturation remanent magnetization (right) upon temperature (Nagata et al., 1974).
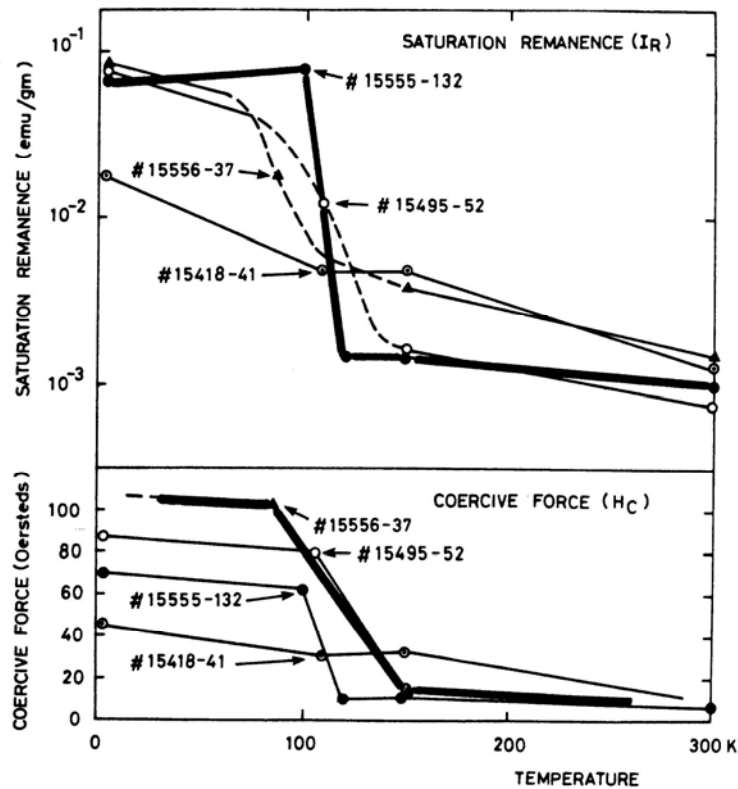

Figure 9. Dependence of the saturation remanent magnetization (top) and the coercive force (bottom) for 15556 (heavy line) and other Apollo 15 samples (Nagata et al., 1974).
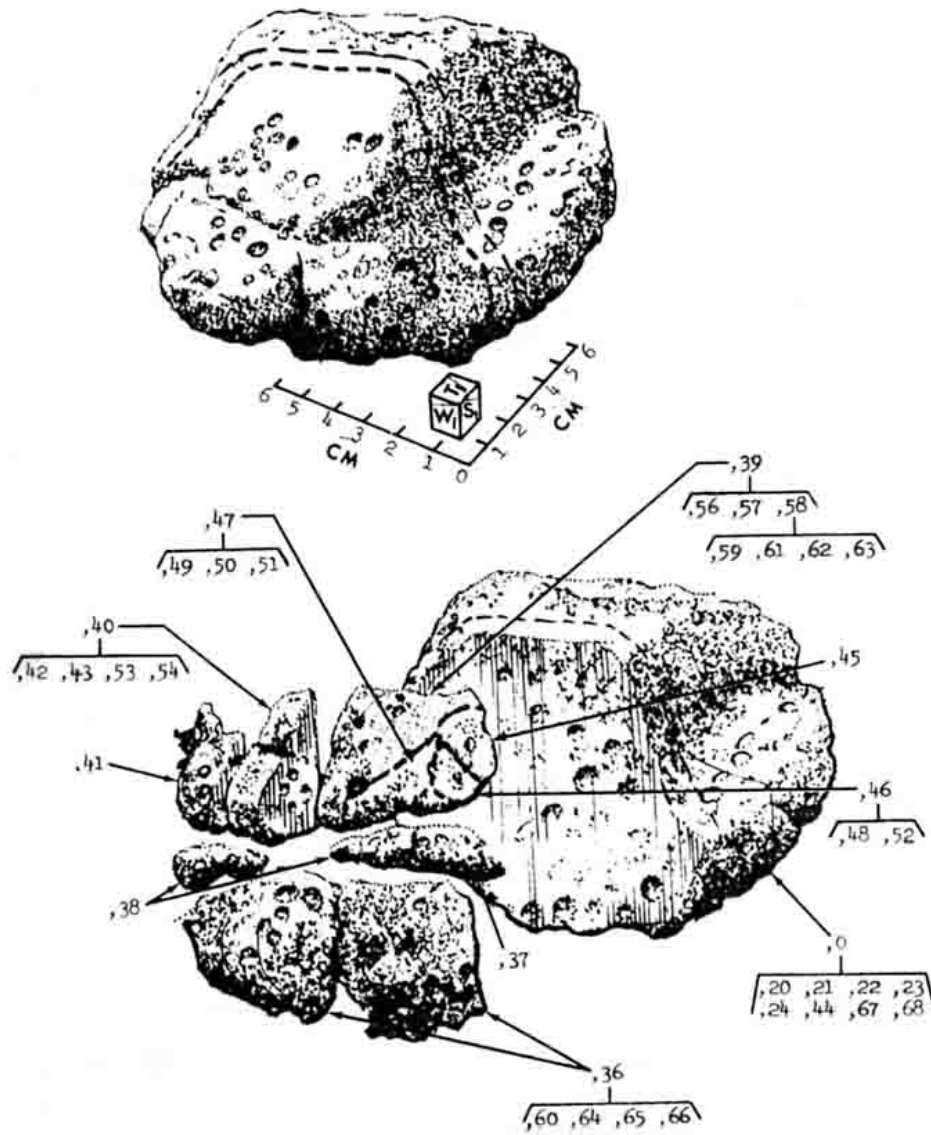
Figure 10. Sawing of 15556. The slab produced in the
1981 sawing is roughly indicated with a dashed line.

TABLE 15556-3 Thin sections of 15556

POTTED BUTT	RELATION TO VESICLES	THIN SECTIONS
,3	Middle ?	,15,18,19,32,34,35,136,137,138
,10	Middle ?	,16,28,29,30,31
,112	Middle	,129,131
,113	Bottom, large vesicle	,130
,116	Top, small vesicles	,132
,128	Middle	,133